# Mechanochemical Synthesis and Nitrogenation of the Nd$_{1.1}$Fe$_{10}$CoTi Alloy for Permanent Magnet

**Hugo Martínez Sánchez** [1,*] **, George Hadjipanayis** [2] **, Germán Antonio Pérez Alcázar** [1,3] **, Ligia Edith Zamora Alfonso** [1,3] **and Juan Sebastián Trujillo Hernández** [1,4]

[1] Departamento de Física, Universidad del Valle, Meléndez, Cali A.A. 25360, Colombia; german.perez@correounivalle.edu.co (G.A.P.A.); ligia.zamora@correounivalle.edu.co (L.E.Z.A.); juan.trujillo@unibague.edu.co (J.S.T.H.)

[2] Department of Physics and Astronomy, University of Delaware, 217 Sharp Lab, Newark, DE 19716, USA; hadji@udel.edu

[3] Centro de Excelencia en Nuevos Materiales (CENM), Universidad del Valle, Meléndez, Cali A.A. 25360, Colombia

[4] Facultad de Ciencias Naturales y Matemáticas, Universidad de Ibagué, Ibagué 730007, Colombia

* Correspondence: martinez.hugo@correounivalle.edu.co

**Abstract:** In this work, the mechanochemical synthesis method was used for the first time to produce powders of the nanocrystalline Nd$_{1.1}$Fe$_{10}$CoTi compound from Nd$_2$O$_3$, Fe$_2$O$_3$, Co and TiO$_2$. High-energy-milled powders were heat treated at 1000 °C for 10 min to obtain the ThMn$_{12}$-type structure. Volume fraction of the 1:12 phase was found to be as high as 95.7% with 4.3% of a bcc phase also present. The nitrogenation process of the sample was carried out at 350 °C during 3, 6, 9 and 12 h using a static pressure of 80 kPa of N$_2$. The magnetic properties M$_r$, μ$_0$H$_c$, and (BH)$_{max}$ were enhanced after nitrogenation, despite finding some residual nitrogen-free 1:12 phase. The magnetic values of a nitrogenated sample after 3 h were M$_r$ = 75 Am$^2$ kg$^{-1}$, μ$_0$H$_c$ = 0.500 T and (BH)$_{max}$ = 58 kJ·m$^{-3}$. Samples were aligned under an applied field of 2 T after washing and were measured in a direction parallel to the applied field. The best value of (BH)$_{max}$ ~ 114 kJ·m$^{-3}$ was obtained for 3 h and the highest μ$_0$H$_c$ = 0.518 T for 6 h nitrogenation. SEM characterization revealed that the particles have a mean particle size around 360 nm and a rounded shape.

**Keywords:** permanent magnets; mechanochemical synthesis; nitrogenation; extrinsic magnetic properties; X-ray diffraction patterns; spin reorientation

## 1. Introduction

The high demand for Nd$_2$Fe$_{14}$B permanent magnets, with maximum energy product (BH)$_{max}$ up to 450 kJ·m$^{-3}$ [1], in applications such as electric vehicles and wind turbines, implies a high production cost owing to the considerable content of Nd. The ferromagnetic R(Fe,M)$_{12}$ compounds, where R is a rare earth element and M is a stabilizing element (V, Ti, Mo, Cr, W, Al or Si), are currently being investigated as alternatives to Nd-Fe-B due to their excellent magnetic properties and their much lower R content [2,3]. It has been found that the ferromagnetic R(Fe,M)$_{12}$ compounds crystalize in the tetragonal ThMn$_{12}$-type structure (space group I4/mmm) with R= Y, Nd, Sm, Gd, Tb, Dy, Ho, Er, Tm or Lu [4], and that these compounds exhibit strong exchange interactions for the light rare earths. The Sm(Fe,M)$_{12}$ compounds are characterized by a strong uniaxial anisotropy [3] and develop a coercive force μ$_0$H$_c$ as high as 1.17 T [5]. The second type of attractive compounds are the Nd(Fe,M)$_{12}$Nx and Pr(Fe,M)$_{12}$Nx with M = Ti, V or Mo [6]. The highest coercivity values for these compounds with a subsequent nitrogenation, μ$_0$H$_c$ up to 1.3 T, have been achieved in nanocrystalline quasi-isotropic alloys with M = Mo [7–10]; somewhat lower μ$_0$H$_c$ values, up to 0.9 T, were reported for nanocrystalline alloys with M = V [11]. Although it is most favorable for a high coercivity, the microstructure of randomly oriented nanograins—usually generated through melt-spinning or high-energy

ball-milling—dramatically lowers the attainable $(BH)_{max}$ due to isotropic nature of the samples. The same alloys (M = Mo, V) also allowed for the synthesis of anisotropic $R(Fe,M)_{12}N_x$ powders with $\mu_0 H_c$ of 0.35–0.58 T [12–16]. No significant coercivity, however, could be developed in the $NdFe_{11}TiN_x$ compound, which is particularly attractive due to the high $M_s$ of 1.48 T [17]; even the $\mu_0 H_c$ reported for the nanocrystalline alloys did not exceed 0.23 T [11]. The mechanochemical synthesis was demonstrated to yield single-crystal submicron and nanoparticles of hard magnetic materials, including the $R(Fe,M)_{12}$ alloys, which exhibit coercivity values typical of nanocrystalline powders [18,19]. This synthesis technique also requires less-expensive oxides, rather than metals, as the raw materials, and it may be expected to reduce local demagnetization fields due to more regular shapes of the particles [20]. The authors are not aware of any reports on mechanochemically synthesized $R(Fe,M)_{12}N_x$ compounds. By reducing nanoscale oxide precursors Su et al. [21] prepared anisotropic $NdFe_{10}Mo_2N_x$ particles, which were a few microns in size and exhibited an $\mu_0 H_c$ of 0.35 T. The aim of this work was to prepare a $Nd(Fe,Co,Ti)_{12}N_x$ permanent magnet material through mechanochemical synthesis and subsequent nitrogenation of the $Nd(Fe,Co,Ti)_{12}$ compound and to study its extrinsic magnetic properties as a function of the temperature and magnetic alignment.

## 2. Materials and Methods

### 2.1. Sample Preparation

The alloy with nominal composition $Nd_{1.1}Fe_{10}CoTi$ was obtained by mechanochemical synthesis, using powders of $Nd_2O_3$ (nominal purity of 99.9%), $Fe_2O_3$ (particles $\leq 5$ μm and 99% purity), $TiO_2$ ($\leq 5$ μm and 99% purity) and Co (1.6 μm and 99.8% purity) as the raw materials. The reactants were mixed with 1 mm granules of Ca (99.5% purity) serving as a reducing agent and CaO powder acting as a dispersant. The amounts of the precursor powders were optimized using a mole ratio (Fe+Co+Ti)/Nd of 6.62 (necessitated by incomplete reduction of the rare earth oxide), and a Ca/O ratio of 2.0 (not counting the CaO dispersant). The mass of the CaO dispersant was three times the mass of the reactants other than Ca. The reactants were first mixed thoroughly with Ca and then with the dispersant. After that, a 5 g charge of the mixed powders was mechanically activated with a Spex-8000 high-energy (University of Delaware, Department of Physics and Astronomy, Sharp Lab, Newark DE, USA) mill by milling for 4 h in argon atmosphere, with six 12 mm steel balls. The subsequent annealing at temperatures from 950 to 1100 °C during 10 min was done in argon-filled quartz capsules, without exposing the as-milled powder to the air. A temperature of 1000 °C was found to be optimal for the formation of the $ThMn_{12}$-type structure. For nitrogenation, the annealed powders were sealed in quartz capsules under 80 kPa of a 99.999%-pure $N_2$ and held at 350 °C for 3, 6, 9 and 12 h. Finally, a multistep procedure of repeated washing with deionized water, glycerol, acetic acid, and ethanol [19] was used to collect the ferromagnetic nitrogenated particles, and to remove the CaO, rare earth oxides and unreacted Ca.

### 2.2. Powder Characterization

The powders were characterized by X-ray diffraction (XRD) in a Rigaku Ultima IV diffractometer (University of Delaware, Department of Physics and Astronomy, Sharp Lab, Newark, DE, USA) with Cu-Kα radiation, and the diffraction patterns were measured in the 2θ range from 25 to 60 degrees. The analysis of XRD patterns was done using the Maud program. Scanning electron microscopy (SEM) was used to study the particle shape and size distribution, using a JEOL JSM-6335F scanning electron microscope (University of Delaware, Department of Physics and Astronomy, Sharp Lab, Newark, DE, USA). The magnetic properties were measured using a Quantum Design VersaLab vibrating sample magnetometer (University of Delaware, Department of Physics and Astronomy, Sharp Lab, Newark DE, USA); the particles were immobilized with paraffin wax, in some cases while applying a 2 T orienting field (hereinafter, "aligned" powders). Correction for

self-demagnetization was done using demagnetization factors experimentally determined for similarly prepared Ni powder.

## 3. Result and Discussion

### 3.1. Structural and Magnetic Characterization before Washing

After the mechanochemical activation and annealing at 1000 °C for 10 min, the powders were characterized by X-ray diffraction and vibrating sample magnetometry. The X-ray diffraction pattern of Figure 1 shows the peaks of the crystalline phases present before washing the powder. The highest peaks correspond to the CaO phase with cubic crystal structure (space group Fm-3m); the phase with $ThMn_{12}$-type crystal structure (space group I4/mmm) or "1:12", is present as a minority phase. The cubic bcc phase (space group Im-3m); and some peaks of the hexagonal $Nd_2O_3$ phase (space group P–63/mmc), as well as of the orthorhombic $CaTiO_3$ phase (space group Pnma) were also identified. The peak at $2\theta = 27.59$ deg possibly corresponds to a rare earth oxide isotypical to $Pr_{24}O_{44}$ (space group P–1).
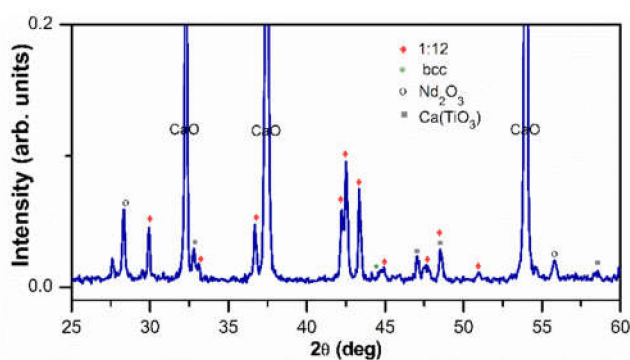


**Figure 1.** X-ray diffraction pattern of the $Nd_{1.1}Fe_{10}CoTi$ powder annealed at 1000 °C for 10 min.

The hysteresis loop of the annealed and not washed powder is shown in Figure 2. Magnetization values at 3 T of 15.67 $Am^2kg^{-1}$, remanence $M_r = 4.43$ $Am^2kg^{-1}$, and $\mu_0H_c = 0.121$ T were obtained by analysis of this measurement. The magnetization values are low due to the predominance of the diamagnetic CaO diluting the ferromagnetic phase-(s). The low $M_r$ and $\mu_0H_c$ values are consistent with the weak anisotropy of nitrogen-free $Nd(Fe,M)_{12}$.
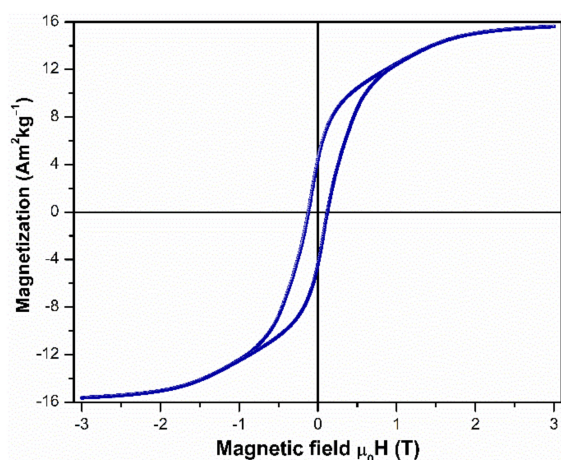


**Figure 2.** Hysteresis loop of the $Nd_{1.1}Fe_{10}CoTi$ powder annealed at 1000 °C for 10 min.

### 3.2. SEM Characterization

Figure 3 shows the SEM images of the washed particles nitrogenated for different times.
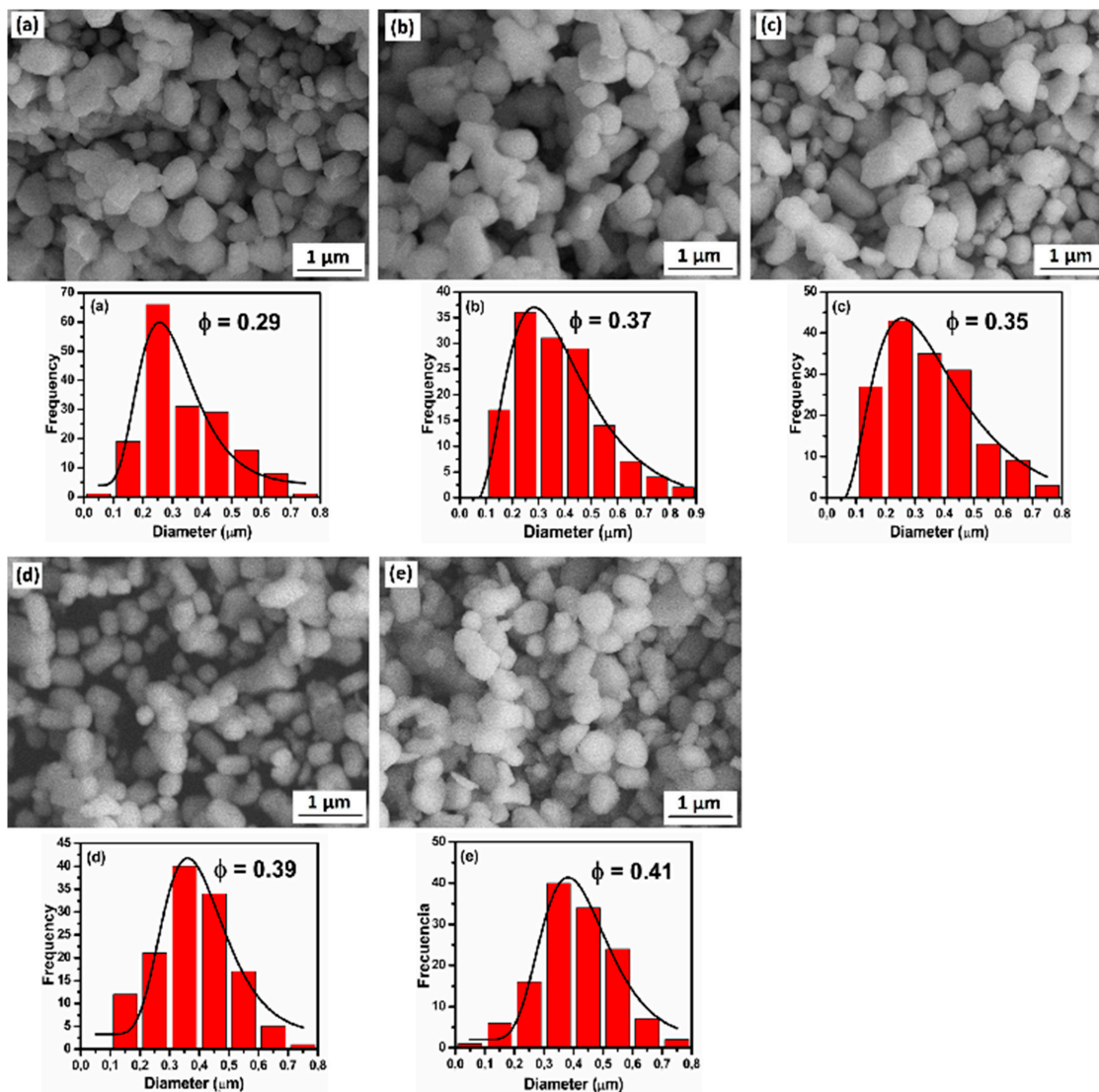


**Figure 3.** SEM micrographs of mechanochemical synthesized of $Nd_{1.1}Fe_{10}CoTi$ particles nitrogenized for (**a**) 0 h, (**b**) 3 h, (**c**) 6 h, (**d**) 9 h and (**e**) 12 h.

The ferromagnetic particles tend to have rounded shape and a log-normal size distribution with a positive asymmetry (Fisher asymmetric coefficient $\gamma_1 > 0$). The log-normal fit showed mean particle sizes of 0.29, 0.37, 0.35, 0.39, and 0.41 μm for the 0, 3, 6, 9, and 12 h nitrogenated samples, respectively. These results show that the particles tend to grow with the increase of nitrogenation time. It is worth noting that the small particle size of about 360 nm and the rounded shape of the particles are important factors for the decrease of the demagnetized field [20] and the improvement of the coercive force.

### 3.3. XRD after Washing

In Figure 4, the XRD diffraction patterns of the washed powders are shown. For the sample without nitrogenation (0 h), the pattern of the peaks of the 1:12 phase, and a single peak of the bcc phase at $2\theta = 44.62$ deg are present. The refinement of the pattern gave a volume fractions of 95.7 and 4.3% for the 1:12 and the bcc phases, respectively. The refined lattice parameters of the 1:12 phase were a = 8.589 Å and c = 4.808 Å. The average crystallite

sizes found from the XRD refinement were 269.7(15.2) nm and 46.4(6.2) nm for the 1:12 and bcc phases, respectively. The mean crystallite size of the 1:12 phase is very close to the value of 0.29 μm obtained for the mean particle size (SEM), indicating that the particles of this phase are single crystals. These single crystal particles lead an improved $\mu_0 H_c$ because of their submicron size.
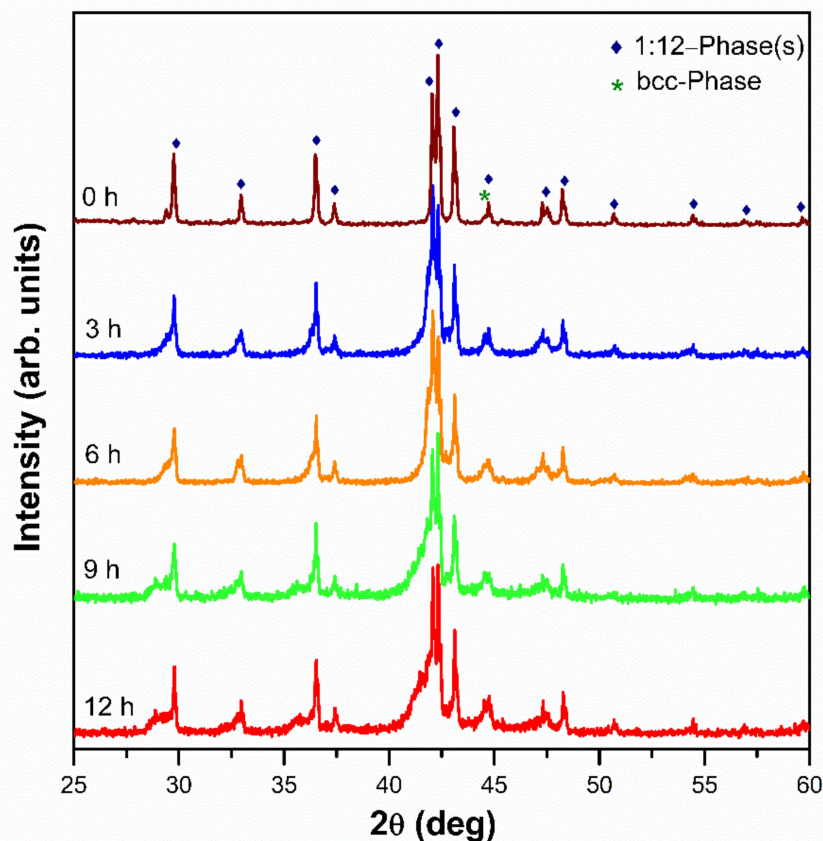


**Figure 4.** X-ray diffraction patterns of $Nd_{1.1}Fe_{10}CoTi$ alloys nitrogenated from 0 to 12 h followed by washing.

The XRD diffractions patterns for the samples nitrogenated for 3, 6, 9 and 12 h do not feature the characteristic shift of the peaks to the left. Instead, the peaks are broadened to their left side as it can be seen in Figure 4. This, apparently, indicates that in all the samples a certain part of the 1:12 phase remains nitrogen-free, even though most of the phase does absorb nitrogen. Thus, the resulting powders may be characterized by a gradient in the N content. In order to verify this hypothesis, Le Bail [22] analysis was carried out, assuming one bcc phase and three distinct 1:12 phases 1:12(a), 1:12(b) and 1:12(c). This analysis allowed for a good refinement of the XRD patterns with the parameters which are presented in Table 1.

The 1:12(a) phase is inherited from the parent, nitrogen-free alloy, because its lattice parameters and unit cell volume are similar, see Table 1. Its XRD peaks are in the right side of the XRD spectrum, as they do not shift to the left upon the nitrogenation. The 1:12(b) and 1:12(c) phases have bigger lattice parameters and therefore bigger volumes of nitrides, indicating that they absorbed different amounts of nitrogen. At the same time, the intensity of the bcc phase peak increases with the nitrogenation time (see Figure 4), indicating that the volume fraction of this phase increases from 4.3 to 8.5% when the nitrogenation time increases from 0 to 12 h.

**Table 1.** Lattice parameters, unit cell volume V, volume fraction and density ρ, for phases in the $Nd_{1.1}Fe_{10}CoTiN_x$ alloys nitrogenated for 0, 3, 6, 9 and 12 h. All data were obtained through refinement of patterns.

| Nitrogenation Time (h) | Phase | *a* (Å) | *c* (Å) | V (Å³) | Fraction (vol. %) | ρ (g/cm³) |
|---|---|---|---|---|---|---|
| 0 | 1:12 | 8.589 | 4.808 | 354.7 | 95.7 | 7.579 |
| | bcc | 2.870 | | | 4.3 | 7.848 |
| 3 | 1:12 (a) | 8.585 | 4.804 | 354.1 | 43.7 | 7.593 |
| | 1:12(b) | 8.631 | 4.843 | 360.8 | 17.7 | 7.452 |
| | 1:12(c) | 8.642 | 4.953 | 369.9 | 34.2 | 7.268 |
| | bcc | 2.870 | | | 4.4 | 7.843 |
| 6 | 1:12(a) | 8.583 | 4.805 | 354.0 | 42.3 | 7.595 |
| | 1:12(b) | 8.616 | 4.849 | 360.0 | 22.4 | 7.469 |
| | 1:12(c) | 8.638 | 4.971 | 370.9 | 29.5 | 7.249 |
| | bcc | 2.871 | | | 5.8 | 7.840 |
| 9 | 1:12(a) | 8.585 | 4.804 | 354.1 | 34.3 | 7.593 |
| | 1:12(b) | 8.631 | 4.843 | 360.8 | 10.0 | 7.452 |
| | 1:12(c) | 8.700 | 4.977 | 376.7 | 48.9 | 7.136 |
| | bcc | 2.873 | | | 6.8 | 7.820 |
| 12 | 1:12(a) | 8.584 | 4.802 | 353.8 | 36.5 | 7.597 |
| | 1:12(b) | 8.642 | 4.841 | 361.5 | 9.5 | 7.436 |
| | 1:12(c) | 8.741 | 4.950 | 378.2 | 45.5 | 7.107 |
| | bcc | 2.871 | | | 8.5 | 7.840 |

Note: Uncertainties for the lattice parameters are ±0.001 Å and for unit cell volume is ±0.16 Å³.

### 3.4. Magnetic Characterization of Aligned and Non-Aligned Powders

Figure 5 presents the hysteresis loops of the randomly oriented $Nd_{1.1}Fe_{10}CoTiN_x$ powders for 0, 3, 6, 9, and 12 h of nitrogenation. The $M_{3T}$, $M_r$ and $\mu_0 H_c$ magnetic properties for the 0 h sample increase after washing from 15.67 to 121.92 $Am^2kg^{-1}$, 4.43 to 57.79 $Am^2kg^{-1}$, and 0.121 to 0.276 T, respectively, due to the removal of non-magnetic CaO and the rare earth oxides. Moreover, the $M_r$ and the $\mu_0 H_c$ values increase after nitrogenation, as it can be seen in the Figure 5 and are listed in Table 2 (in parenthesis). This enhancement of the magnetic properties is due to the interstitial modification of those 1:12 crystallites which absorb nitrogen, leading to enhancement of their magnetocrystalline anisotropy.

The values of $\mu_0 H_c$ decrease when the nitrogenation is increased from 3 to 12 h, apparently, because of a nearly doubled amount of the soft magnetic bcc phase. The $M_r$ = 75.27 $Am^2kg^{-1}$, $\mu_0 H_c$ = 0.500 T, and $(BH)_{max}$ = 58.38 kJ·m⁻³ values for 3 h of nitrogenation are comparable to those reported in [9,23], for isotropic nanocrystalline $Nd(Fe,Mo)_{12}N_x$ alloys, even though 1:12 alloys stabilized with Mo, are known to exhibit a higher coercivity than the 1:12 alloys stabilized with Ti.
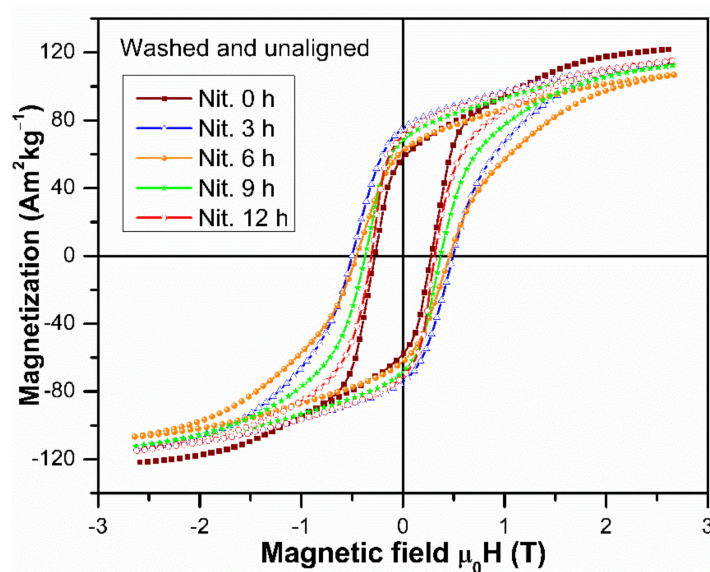
**Figure 5.** Hysteresis loops of the randomly oriented $Nd_{1.1}Fe_{10}CoTiN_x$ alloys after washing as a function of nitrogenation time.

**Table 2.** Magnetic properties of aligned and randomly oriented (in parenthesis) $Nd_{1.1}Fe_{10}CoTiN_x$ powders nitrogenated for the indicated time.

| Nitrogenation Time (h) | $M_{3T}$ $(Am^2kg^{-1})$ | $M_r$ $(Am^2kg^{-1})$ | $\mu_0H_c$ (T) | $(BH)_{max}$ $(kJ \cdot m^{-3})$ |
|---|---|---|---|---|
| 0 | 122.83 (121.92) | 108.21 (57.79) | 0.294 (0.276) | 81.07 (30.44) |
| 3 | 128.80 (114.17) | 116.34 (75.27) | 0.504 (0.500) | 113.74 (58.38) |
| 6 | 128.97 (106.90) | 116.14 (62.16) | 0.518 (0.457) | 111.41 (39.89) |
| 9 | 126.38 (112.45) | 113.24 (68.28) | 0.395 (0.371) | 96.40 (44.02) |
| 12 | 126.97 (115.12) | 112.87 (71.15) | 0.316 (0.312) | 87.85 (45.74) |

Note: Uncertainties for $M_{3T}$, $M_r$, $\mu_0H_c$ and $(BH)_{max}$ are $\pm0.20$ $Am^2kg^{-1}$, $\pm0.14$ $Am^2kg^{-1}$, $\pm0.001$ T and $\pm0.35$ $kJ \cdot m^{-3}$, respectively.

In Figure 6, the hysteresis loops for the anisotropic ferromagnetic particles aligned with an external field are shown; the corresponding $M_{3T}$, $M_r$, $\mu_0H_c$, and $(BH)_{max}$ dates are listed in Table 2 (without parenthesis). All the hard magnetic properties were found to be enhanced by the alignment. It is obvious that the increase of $M_{3T}$ and $M_r$ is the immediate result of the easy axes of the crystallites being aligned with the direction of the measurements. The improvement of $\mu_0H_c$ is caused by the increase of the magnetocrystalline anisotropy due to the nitrogenization. The reduced remanence $M_r/M_{3T}$ increases upon nitrogenation and the alignment; for 3, 6 and 9 h of nitrogenation, a value of 0.90 was obtained despite the soft magnetic bcc phase. The possibility to align the easy axes of magnetization in the $Nd(Fe,M)_{12}N_x$ particles is important for the development of high $(BH)_{max}$ values, as it is shown in Table 2. A $(BH)_{max} = 113.74$ $kJ \cdot m^{-3}$ that was obtained for the aligned particles after nitrogenation for 3 h is the highest $(BH)_{max}$ value reported so far for the $Nd(Fe,M)_{12}N_x$ compounds, and it contributes to closing the gap between the hexaferrites and the "RE-lean" magnets [1]. Moreover, this $(BH)_{max}$ value is better than those reported for $NdFe_{9.4}Co_{1.6}MoN_x$ [9], Mn-Al-C [24], and MnBi [25], that are 56.50, 73.21, and 70.82 $kJ \cdot m^{-3}$, respectively.
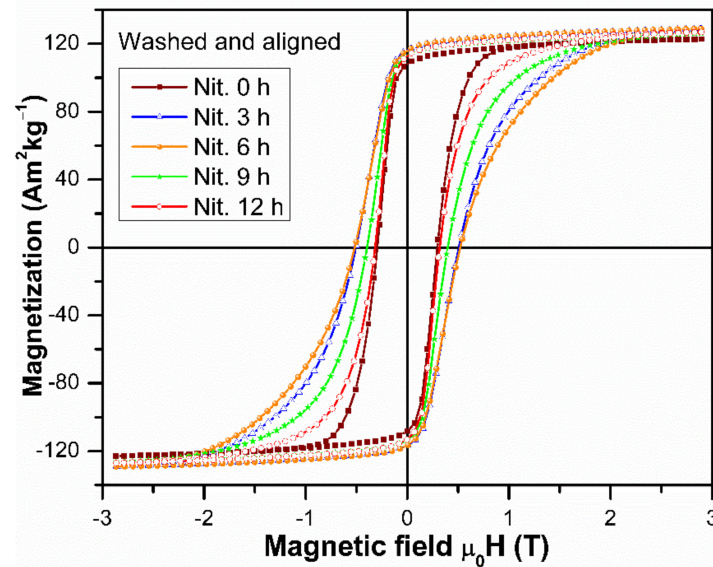
**Figure 6.** Hysteresis loops of the $Nd_{1.1}Fe_{10}CoTiN_x$ alloys nitrogenized for the indicated time, washed, and magnetically oriented.

### 3.5. Magnetic Characterization at Low Temperatures

To study the evolution of $M_{3T}$, $M_r$, and $\mu_0H_c$ with the temperature, the hysteresis loops were measured in the first and the second quadrant, for the sample nitrogenated at 6 h, as can see in Figure 7. The 6 h nitrogenation was selected because it exhibited one of the best magnetic properties after nitrogenation without alignment. The strong uniaxial anisotropy of the $R(Fe,Ti)_{12}$ compounds has been associated with the strong coupling of both rare earth and transition metal magnetic sublattices, which favor an axial orientation [26]. However, experimental and theoretical studies have shown that for the $NdFe_{11}Ti(N$ or $H)$ compounds, a rotation of the easy axis anisotropy to a canted or basal orientation with the decrease of the temperature is obtained, and this behavior is known as spin reorientation [4,27,28].
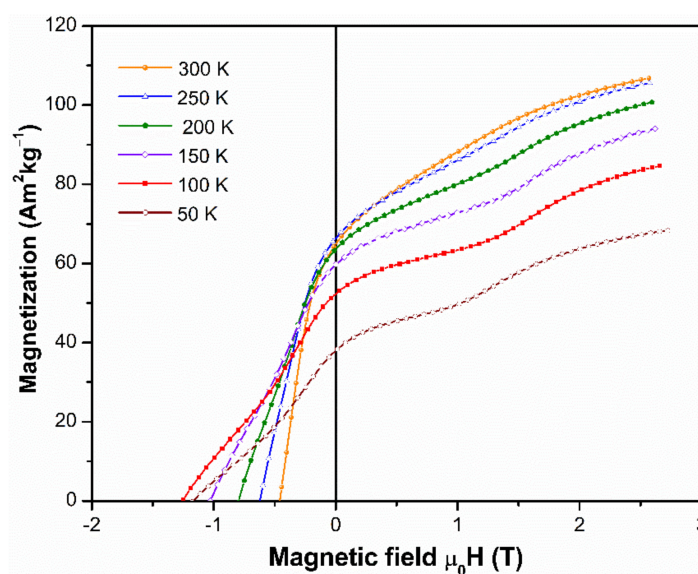


**Figure 7.** Demagnetization curves of $Nd_{1.1}Fe_{10}CoTiN_x$ powder nitrogenated during 6 h and washed. The specimen was not magnetically oriented.

Temperature dependence of magnetization of the $NdFe_{11}Ti$ compound reported a peak at ~200 K related to the spin reorientation of this compound [4]. In aligned powders, a maximum of magnetization was observed at temperatures higher than the spin reorientation temperature [29]. The decrease of M(H) as a function of temperature shown in Figure 7 can be associated with the spin reorientation. The jumps of magnetization emerging in the 1st M(H) quadrant with the decrease of temperature can also be attributed to a metamagnetic spin reorientation transition [30]. The $M_{3T}$, $M_r$, and $\mu_0 H_c$ values are shown in Figure 8 as a function of the temperature.
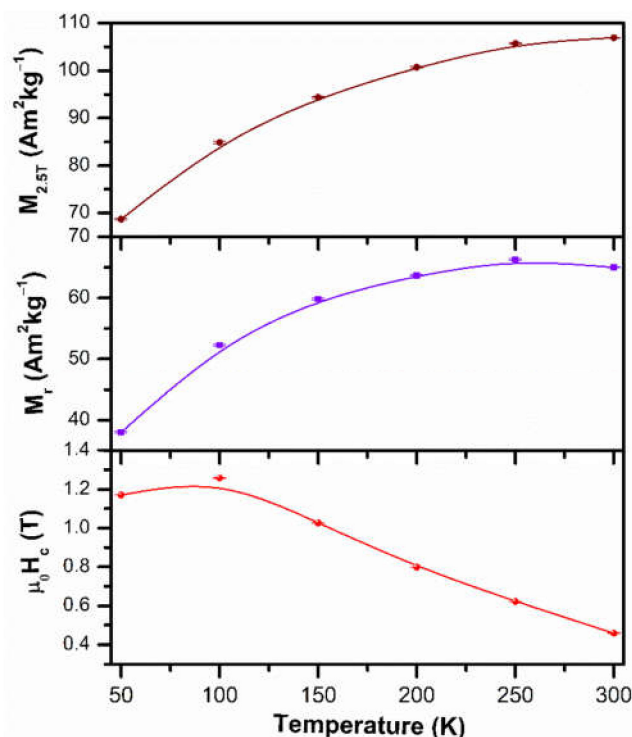


**Figure 8.** Saturation magnetization, remanence and coercivity $Nd_{1.1}Fe_{10}CoTiN_x$ alloy nitrogenated during 6 h and as a function of temperature. The specimen was not magnetically oriented.

For the $\mu_0 H_c$, a tendency to increase with the decrease in the temperature is shown in Figure 8; A maximum value of $\mu_0 H_c = 1.259$ T was obtained at 100 K. This fact indicates that the spin-reorientation transition occurs around this temperature, in agreement with the reported spin-reorientation temperature for the $NdFe_{11}TiH$ compound (100 K [27]). On the other hand, this change in the $\mu_0 H_c$ with the decrease of the temperature was also observed in the $(Nd_{0.2}Ce_{0.8})_2Fe_{14}B$ compound at 100 K, where it was similarly associated with the spin-reorientation temperature [31]. For the lower temperature of 50 K, the $\mu_0 H_c$ decreases to 1.171 T as can be seen in Figure 8.

## 4. Conclusions

The mechanochemical synthesis has been demonstrated to be a powerful technique to synthetize submicron single crystal $Nd(Fe,Co,Ti)_{12}N_x$ particles with rounded shape, and reasonably good magnetic properties. The nitrogenated $Nd_{1.1}Fe_{10}CoTiN_x$ compounds exhibited a significant improvement of their magnetic properties after being washed, and aligned, even though according to the Le Bail analysis of the XRD patterns about 40 vol.% of the original 1:12 phase, did not adsorb nitrogen in this experiment. The increase in the magnetic properties $M_r$, $\mu_0 H_c$ and $(BH)_{max}$ upon nitrogenation results in values of 75 $Am^2 kg^{-1}$, 0.500 T and 58 $kJ \cdot m^{-3}$, respectively, for the sample with 3 h of nitrogenation. Comparison of the XRD analysis of the crystallite size and SEM characterization of the

particles revealed that the washed 1:12 particles were monocrystalline. The alignment of the samples with an external magnetic field appears to be a very important factor to significantly enhance the magnetic properties. The best $(BH)_{max} \sim 114$ kJ·m$^{-3}$ was measured for the sample with 3 h of nitrogenation, thus significantly improving the values previously reported for other systems. The best $\mu_0 H_c = 0.518$ T was obtained in a sample with 6 h of nitrogenation. Low temperature M(H) curves show magnetization jumps, which indicate a first order magnetization process.

**Author Contributions:** Conceptualization, H.M.S., G.H., G.A.P.A.; methodology, H.M.S., G.H., L.E.Z.A., J.S.T.H.; software, H.M.S., J.S.T.H.; validation, H.M.S., G.H., G.A.P.A., L.E.Z.A., J.S.T.H.; formal analysis, H.M.S.; investigation, H.M.S.; writing—original draft preparation, H.M.S.; writing—review and editing, H.M.S., G.H., G.A.P.A., L.E.Z.A., J.S.T.H.; supervision, G.H., G.A.P.A., L.E.Z.A., J.S.T.H.; project administration, G.A.P.A., G.H.; funding acquisition, J.S.T.H., G.A.P.A. All authors have read and agreed to the published version of the manuscript.

**Institutional Review Board Statement:** Not applicable.

**Informed Consent Statement:** Not applicable.

**Data Availability Statement:** The data that support the results of this research are available when the editorial office of this journal requires it.

**Conflicts of Interest:** The authors declare no conflict of interest.

## References

1. Madugundo, R.; Rama Rao, N.V.; Schönhöbel, A.M.; Salazar, D.; El-Gendy, A.A. Recent Developments in Nanostructured Permanent Magnet Materials and Their Processing Methods. In *Magnetic Nanostructured Materials: From Lab to Fab*; Elsevier: Amsterdam, The Netherlands, 2018. [CrossRef]
2. Tukker, A. Rare earth elements supply restrictions: Market failures, not scarcity, hamper their current use in high-tech applications. *Environ. Sci. Technol.* **2014**, *48*, 9973–9974. [CrossRef] [PubMed]
3. Schönhöbel, A.M.; Madugundo, R.; Vekilova, O.Y.; Eriksson, O.; Herper, H.C.; Barandiarán, J.M.; Hadjipanayis, J.C. Intrinsic magnetic properties of SmFe$_{12-x}$V$_x$ alloys with reduced V-concentration. *J. Alloys Compd.* **2019**, *786*, 969–974. [CrossRef]
4. Hu, B.P.; Li, H.S.; Gavigan, J.P.; Coey, J.M.D. Intrinsic magnetic properties of the iron-rich ThMn$_{12}$-structure alloys R(Fe$_{11}$Ti); R=Y, Nd, Sm, Gd, Tb, Dy, Ho, Er, Tm and Lu. *J. Phys. Condens. Matter* **1989**, *1*, 755–770. [CrossRef]
5. Schultz, L.; Schnitzke, K.; Wecker, J. High coercivity in mechanically alloyed Sm-Fe-V magnets with a ThMn$_{12}$ crystal structure. *Appl. Phys. Lett.* **1990**, *56*, 1376–1378. [CrossRef]
6. Yang, J.; Yang, Y. Magnetic properties and interstitial atom effects in the R(Fe,M)$_{12}$ compounds. In *Handbook of Advanced Magnetic Materials*; Springer: Boston, MA, USA, 2006; pp. 1414–1451.
7. Yang, J.; Oleinek, P.; Müller, K.H. Hard magnetic properties of melt-spun R(Fe,M)$_{12}$ nitrides (R= Nd or Pr; M= Mo or V). *J. Appl. Phys.* **2000**, *88*, 988–992. [CrossRef]
8. Zhang, X.D.; Cheng, B.P.; Yang, Y.C. High coercivity in mechanically milled ThMn$_{12}$-type Nd–Fe–Mo nitrides. *Appl. Phys. Lett.* **2000**, *77*, 4022–4024. [CrossRef]
9. Liu, S.; Han, J.; Du, H.; Wang, C.; Yang, Y.; Yang, J.; Chang, H. High energy product in mechanically alloyed ThMn$_{12}$-type compound with exchange coupling effect. *J. Magn. Magn. Mater.* **2007**, *312*, 449–452. [CrossRef]
10. Lin, Z.; Han, J.; Liu, S.; Xing, M.; Yang, Y.; Yang, J.; Wang, C.; Dua, H.; Yang, Y. Phase composition, microstructures and magnetic properties of melt-spun Nd$_{1.2}$Fe$_{10.5}$Mo$_{1.5}$ ribbons and their nitrides. *J. Magn. Magn. Mater.* **2012**, *324*, 196–199. [CrossRef]
11. Tang, S.L.; Wu, C.H.; Jin, X.M.; Wang, B.W.; Li, G.S.; Ding, B.Z.; Chuang, Y.C. Phase formation and magnetic properties of annealed mechanical alloying Nd-Fe-V-Ti alloys and their nitrides; *J. Alloys Compd.* **1998**, *264*, 240–243. [CrossRef]

12. Yang, J.; Mao, W.; Yang, Y.; Ge, S.; Zhao, Z.; Li, F. Nitrogenation of the magnetic compound R(Fe,M)$_{12}$. *J. Appl. Phys.* **1998**, *83*, 1983–1987. [CrossRef]
13. Mao, W.; Zhang, X.; Ji, C.; Chang, H.; Cheng, B.; Yang, Y.; Du, H.; Xue, Y.; Zhang, B.; Wang, L.; et al. Structural and magnetic properties of PrFe12-xVx and their nitrides. *Acta Mater* **2001**, *49*, 721–728. [CrossRef]
14. Han, J.; Liu, S.; Xing, M.; Lin, Z.; Kong, X.; Yang, J.; Wang, C.; Du, H.; Yang, Y. Preparation of anisotropic Nd(Fe,Mo)$_{12}$N$_{1.0}$ magnetic materials by strip casting technique and direct nitrogenation for the strips. *J. Appl. Phys.* **2011**, *109*, 07A738. [CrossRef]
15. Yang, Y.; Yang, J.; Han, J.; Wang, C.; Liu, S.; Du, H. Research and development of interstitial compounds. *IEEE Trans. Magn.* **2015**, *51*, 2103806. [CrossRef]
16. Fu, J.B.; Yu, X.; Qi, Z.Q.; Yang, W.Y.; Liu, S.Q.; Wang, C.S.; Du, H.L.; Han, J.Z.; Yang, Y.C.; Yang, J.B. Magnetic properties of Nd(Fe$_{1-x}$Co$_x$)$_{10.5}$M$_{1.5}$ (M = Mo and V) and their nitrides. *AIP Adv.* **2017**, *7*, 056202. [CrossRef]
17. Akayama, M.; Fujii, H.; Yamamoto, K.; Tatami, K. Physical properties of nitrogenated RFe$_{11}$Ti intermetallic compounds (R = Ce, Pr and Nd) with ThMn$_{12}$-type structure. *J. Magn. Magn. Mater.* **1994**, *130*, 99–107. [CrossRef]
18. Gabay, A.M.; Hadjipanayis, G.C. Mechanochemical synthesis of magnetically hard anisotropic RFe$_{10}$Si$_2$ powders with R representing combination of Sm, Ce and Zr. *J. Magn. Magn. Mater.* **2017**, *422*, 43–48. [CrossRef]
19. Gabay, A.M.; Martín-Cid, A.; Barandiaran, J.M.; Salazar, D.; Hadjipanayis, G.C. Low-cost Ce$_{1-x}$Sm$_x$(Fe,Co,Ti)$_{12}$ alloys for permanent magnets. *AIP Adv.* **2016**, *6*, 056015. [CrossRef]
20. Dirba, I.; Li, J.; Sepehri-Amin, H.; Ohkubo, T.; Schrefl, T.; Hono, K. Anisotropic, Single-crystalline SmFe$_{12}$-based microparticles with high roundness fabricated by jet-milling. *J. Alloys Compd.* **2019**, *804*, 155–162. [CrossRef]
21. Su, M.Z.; Liu, S.F.; Qian, X.L.; Lin, J.H. An alternative approach to the finely crystalline powder of rare earth-transition metal alloys: *J. Alloys Compd.* **1997**, *249*, 229–233. [CrossRef]
22. Le Bail, A.; Duroy, H.; Fourquet, J.L. Ab-initio structure determination of LiSbWO$_6$ by X-ray powder diffraction. *Mater. Res. Bull.* **1988**, *23*, 447–452. [CrossRef]
23. Aubert, A.; Madugundo, R.; Schönhöbel, A.M.; Salazar, D.; Garitaonandia, J.S.; Barandiaran, J.M.; Hadjipanayis, G. Structural and magnetic properties of Nd-Fe-Mo-(N) melt-spun ribbons with ThMn$_{12}$ structure. *Acta Mater.* **2020**, *195*, 519–526. [CrossRef]
24. Kubo, T.; Ohtani, T.; Kojima, S.; Kato, N.; Kojima, K.; Sakamoto, Y.; Tsukahara, M. Machinable Anisotropic Permanent Magnets of Mn-Al-C Alloys. U.S. Patent 3, 976, 519, 24 August 1976.
25. Yang, J.; Yang, W.; Shao, Z.; Liang, D.; Zhao, H.; Xia, Y.; Yang, Y. Mn-based permanent magnets. *Chin. Phys. B.* **2018**, *27*, 117503. [CrossRef]
26. Boltich, E.B.; Ma, B.M.; Zhang, L.Y.; Pourarian, F.; Malik, S.K.; Sankar, S.G.; Wallace, W.E. Spin reorientations in RTiFe$_{11}$ systems (R = Tb, Dy and Ho). *J. Magn. Magn. Mater.* **1989**, *78*, 364–370. [CrossRef]
27. Piquer, C.; Grandjean, F. A magnetic and Mössbauer spectral study of the spin reorientation in NdFe$_{11}$Ti and NdFe$_{11}$TiH. *J. Appl. Phys.* **2004**, *95*, 6308–6316. [CrossRef]
28. Guslienko, K.Y.; Kou, X.C.; Grössinger, R. Magnetic anisotropy and spin-reorientation transitions in RFe$_{11}$Ti (R= Nd, Tb, Dy, Er) rare-earth intermetallics, *J. Magn. Magn. Mater.* **1995**, *150*, 383–392. [CrossRef]
29. Luong, N.H.; Thuy, N.P.; Tal, L.T.; Hoang, N.V. Effect of Y substitution of the spin reorientation in NdFe$_{11}$Ti compound. *Phys. Status Solidi* **1990**, *121*, 607–610. [CrossRef]
30. Pateti, L.; Paoluzi, A.; Albertini, F. Magnetic anisotropy and magnetization processes in 3:29 and 1:12 Nd(FeTi)-based compounds. *J. Appl. Phys.* **1994**, *76*, 7473–7477. [CrossRef]
31. Kolchugina, N.B.; Zheleznyi, M.V.; Savchenko, A.G.; Menushenkov, V.P.; Burkhanov, G.S.; Koshkid'ko, Y.S.; Ćwik, J.; Dormidontov, N.A.; Skotnicova, K.; Kursa, M.; et al. Simulating the hysteretic characteristics of hard magnetc materials based on Nd$_2$Fe$_{14}$B and Ce$_2$Fe$_{14}$B intermetallics. *Crystals* **2020**, *10*, 518. [CrossRef]